Land cover change dominates decadal trends of biogenic volatile organic compound (BVOC) emission in China

Hui Wang[1, 2], Qizhong Wu[1], Alex B. Guenther[2], Xiaochun Yang[1], Lanning Wang[1], Tang Xiao[3], Jie Li[3], Jinming Feng[4], Qi Xu[1], Huaqiong Cheng[1]

[1]College of Global Change and Earth System Science, Joint Center for Global Changes Studies, Beijing Normal University, Beijing 100875, China
[2]Department of Earth System Science, University of California, Irvine, CA 92697, USA
[3]State Key Laboratory of Atmospheric Boundary Layer Physics and Atmospheric Chemistry, Institute of Atmospheric Physics, Chinese Academy of Sciences, Beijing 100029, China
[4]Key Laboratory of Regional Climate-Environment for Temperate East Asia, Institute of Atmospheric Physics, Chinese Academy of Sciences, Beijing 100029, China
Correspondence to: Qizhong Wu (wqizhong@bnu.edu.cn) & Lanning Wang (wangln@bnu.edu.cn)

Abstract. Satellite observations reveal that China has been leading the global greening trend in the past two decades. We assessed the impact of land cover change on total BVOC emission in China during 2001-2016 and found a significant increasing trend of 1.09% yr-1 with increases of 1.35, 1.25 and 1.43 % yr-1 for isoprene, monoterpenes and sesquiterpenes, respectively. Comparison of different scenarios showed that vegetation change is the main driver of BVOC emission change in China. Considerable heterogeneity was observed on regional scales, with the highest increasing trends of BVOC emission found in the Qinling Mountains and in the south of China. The BVOC emission for the year 2016 in these two regions was enhanced by 61.89 and 67.64% compared to that of 2001, respectively. We compared the long-term HCHO vertical columns (VC) from the satellite-based Ozone Monitoring Instrument (OMI) with the estimation of isoprene emission in summer. The results showed statistically significant positive correlation coefficients over the regions with high vegetation cover fractions. In addition, the isoprene emission and HCHO VC both showed statistically significant increasing trends in the south of China where these two variables have high positive correlation coefficients. This result supports our estimation of the variability and trends of BVOC emission in China. Although anthropogenic sources comprise ~63% NMVOC emissions in China, the continued increase of BVOC will enhance the importance of considering BVOC when making policies for controlling ozone pollution in China along with ongoing efforts to reduce anthropogenic emissions.

1 Introduction

Biogenic Volatile Organic Compounds (BVOCs) play an important role for air quality and the climate system due to their large emission amount and reactivity (Guenther et al., 1995; Guenther, 2006). BVOCs are important precursors of ozone and secondary organic aerosols (SOAs) (Kavouras et al., 1998; Claeys et al., 2004), therefore, it is important to understand the variability of BVOC emission and its impact on

air quality and the climate system. The emission of BVOC is controlled by multiple environmental factors like temperature, radiation, concentration of CO_2 and other stresses, and is affected by climate changes (Guenther et al., 1995; Arneth et al., 2007; Penuelas and Staudt, 2010). Besides the climatic factors, the land cover change also plays a key role in the variability of BVOC emission (Stavrakou et al., 2014;

5   Unger, 2014;Chen et al., 2018), e.g., cropland expansion has been estimated to dominate the reduction of isoprene, the dominant BVOC species, in last century (Lathière et al., 2010; Unger, 2013) although there are large uncertainties associated with these estimates.

China has been greening in recent decades (Piao et al., 2015). A recent study points out that China accounts for 25% of the net increase of global leaf area during 2000-2017 (Chen et al., 2019). The increase

10   of forest area plays a dominant role in greening in China with multiple programs to maintain and expand forests (Zhang et al., 2016; Bryan et al., 2018; Chen et al., 2019). The enhancement of vegetation cover rate and biomass can lead to the increase of BVOC emission in China and induce a corresponding impact on local air quality and the climate system. Previous studies have investigated the long-term emission trend of dominant BVOC species like isoprene in China (Fu and Liao, 2012; Li and Xie, 2014; Stavrakou

15   et al., 2014; Chen et al., 2019). Li and Xie (2014) estimated the historical BVOC emissions during 1981-2003 in China using the national forest inventory records and reported that the BVOC emission increased at a rate of 1.27% yr-1. Another estimation by Stavrakou et al. (2014) showed an upward trend of 0.42% yr-1 of isoprene emission in China during 1979-2005 driven by the increasing temperature and solar radiation, moreover, the upward trend of isoprene emission reached 0.7% yr-1 when considering the

20   replacement of cropland with forest. A recent study by Chen et al. (2018) concluded that the global isoprene emission decreased by 1.5% because of the tree cover change during 2000-2015, but in China, the isoprene emitted by broadleaf trees and non-trees increased by 3.6% and 5.4%, respectively. However, these studies have limitations in representing annual changes of vegetation, e.g., Li and Xie (2014) used fixed LAI input of year 2003 over the whole study period of 1981-2003.

25   Considering the significant land cover change and greening trend in China, it is necessary to thoroughly investigate the impact of intense reforestation on BVOC emission in China. In this study, we used the latest annually continuous land cover products Version 6 by the MODerate-resolution Imaging Spectroradiometer (MODIS) sensors as well as the Model of Emissions of Gases and Aerosols from

Nature (MEGAN, Guenther et al. 2012) model to investigate BVOC emission in China from 2001 to 2016. By annually updating the vegetation information of MODIS observations, we could accurately estimate interannual variability of BVOC emission to assess the impact of greening trend on BVOC in China during 2001-2016.

5   There are no long-term in-situ observation of BVOC in China to validate our estimation of interannual variability of BVOC emission, however, satellite formaldehyde (HCHO) observations provide an opportunity to validate the interannual variability of isoprene, the dominant compound among BVOC species that accounts for almost half of total BVOC emission in China (Li et al., 2013). Since HCHO is an important proxy of isoprene in forest regions with no significant anthropogenic impact, satellite

10 observed HCHO columns are widely used to derive regional ecosystem isoprene emission (Palmer et al., 2003; Marais et al., 2012; Stavrakou et al., 2015; Kaiser et al. 2018). Zhu et al. (2017b) reported the increasing trend of HCHO vertical columns (VC) detected by Ozone Monitoring Instrument (OMI) driven by increasing cover rate of local forest in the northwestern US. Stavrakou et al. (2018) also used the long-term HCHO VC to investigate the annual variability of BVOC induced by climate variability. We have

15 used the long-term HCHO record from 2005-2016 by OMI to assess our estimation of annual isoprene variability.

2 Data and Method

2.1 MEGAN Model

MEGAN (Guenther et al., 2006) is the most widely used model for calculating BVOC emission from

20 regional to global scales (Müller et al., 2008; Li et al., 2013; Sindelarova et al., 2014; Chen et al., 2018). The offline version of the MEGAN v2.1 (Guenther et al., 2012) model, available at https://bai.ess.uci.edu/megan, was used to estimate the BVOC emission in China from 2001 to 2016. MEGAN v2.1 calculates emissions for 19 major compound categories using fundamental algorithm:

$$F_i = \varepsilon_i \gamma_i \qquad (1)$$

where Fi, εi and γi represent the emission amount, standard emission factor and emission activity factor of chemical species i. The standard emission factor in this study is based on the plant functional type (PFT) distribution, and the PFT scheme in MEGAN v2.1 is the scheme adopted in Community Land Model 4.0 (Lawrence et al., 2011). The emission activity factor γi accounts for the impact of multiple environmental factors and expresses it as:

$$\gamma_i = C_{CE} LAI \gamma_{p,i} \gamma_{T,i} \gamma_{A,i} \gamma_{SM,i} \gamma_{C,i} \tag{2}$$

where $\gamma_{p,i}$, $\gamma_{T,i}$ $\gamma_{A,i}$ $\gamma_{SM,i}$ and $\gamma_{C,i}$ represent the activity factors for light, temperature, leaf age, soil moisture and CO_2 inhibition impact. The Cce (=0.57) is a factor to set the γi equal to 1 at the standard conditions. The LAI is the leaf area index and defines the amount of foliage and the leaf age in MEGAN. The light and temperature response algorithms in MEGAN v2.1 are from Guenther et al. (1991), Guenther et al. (1993) and Guenther et al. (2012), which described enzymatic activities controlled by temperature and light conditions. The CO_2 inhibition algorithm is from Heald et al. (2009), and only the estimation of isoprene emission considers the impacts of soil moisture and CO_2 concentration. The detailed descriptions of these factor algorithms can be found in Guenther et al. (2012) and Sakulyanontvittaya et al. (2008).

2.2 Land Cover Datasets.

The land cover parameters for driving MEGAN including LAI, PFT and vegetation cover fraction (VCF) were provided by satellite datasets. The MODIS MOD15A2H for 2001 and MCD15A2H for 2002-2016 LAI datasets were adopted in this study. The parameter LAIv in MEGAN is calculated as:

$$LAIv = \frac{LAI}{VCF} \tag{3}$$

where VCF is provided by MODIS MOD44B datasets.

The PFT was used to determine the canopy structure and standard emission factors in MEGAN (Guenther et al., 2012). The PFT data in this study is obtained from the MODIS MCD12C1 land cover product, and MODIS PFT classification were converted to MEGAN PFT classification based on the climatic criteria described by Bonan Gordon et al. (2002) using the climatology of ERA-interim dataset (Berrisford et al.,

2011) during 2001-2016. We adopted the default emission factors of different PFTs described in Guenther et al. (2012).

2.3 Meteorological Datasets

The hourly meteorological fields were provided by the Weather Research and Forecast (WRF) Model V3.9 (Skamarock et al., 2008) simulations. The meteorological simulation is driven by ERA-Interim reanalysis data (Berrisford et al., 2011) with 27 km horizontal spatial resolution and 39 vertical layers. The physical schemes were presented in supplemental Table S1.

Since light and temperature conditions are the main environmental drivers of BVOC emission (Guenther et al., 1993; Sakulyanontvittaya et al., 2008), we assessed the reliability of the WRF simulated downward shortwave radiation (DSW) and 2-meter temperature (T2) using the in-situ observations from 98 radiation observation sites and 697 meteorology observation sites in China. The in-situ observations used in this study are from the National Meteorological Information Center (http://data.cma.cn/). We converted the hourly model outputs and daily observations to monthly average values from 2001 to 2016 for comparison. For DSW, the average mean bias (MB), mean error (ME) and root mean square error (RMSE) are 40.37 (± 20.81), 43.55 (± 17.52) and 49.79 (± 17.70) W m-2 among 98 sites, and the overestimation of DSW simulation is a common issue in multiple simulation studies and may be induced by the lack of aerosol radiation affect and cloud simulation (Wang et al., 2011; Situ et al., 2013; Wang et al., 2018). For T2, the average MB, ME and RMSE are -1.19 (± 2.87), 2.40 (± 2.14) and 2.65 (± 2.11) °C among 697 sites over China. We also compared the monthly anomalies of DSW and T2 from the model simulation and observation to validate the interannual variability of meteorological fields simulated by WRF. As shown in Figure 1, the results indicate that the model accurately reproduced the interannual variability of DSW and T2, and the correlation coefficients of DSW and T2 anomaly between the simulation and observation reached 0.77 and 0.88, respectively. Our WRF simulation successfully captured the long-term meteorological variabilities and is reasonable to use for estimating the impact of climatic variability on BVOC emission in China for this study.

2.4 Satellite Formaldehyde Observation

The satellite HCHO VC used in this study is from the Belgian Institute for Space Aeronomy (BIRA-IASB) and retrieved using the differential optical absorption spectroscopy (DOAS) algorithm (De Smedt et al., 2012; De Smedt et al., 2015). The detailed description of the BIRA-IASB OMI HCHO product can be found in De Smedt et al. (2015), and we used the monthly HCHO VC with $0.25° \times 0.25°$ spatial resolution. Since the OMI instrument is temporally stable (Dobber et al., 2008; De Smedt et al., 2015), the OMI HCHO VC product is suitable for long-term analysis (Jin and Holloway, 2015) and was used to primarily validate our estimation of isoprene emission variability. The major sources of tropospheric HCHO are biogenic VOC, anthropogenic source and open fires (Zhu et al., 2017a). Since biogenic isoprene is the dominant source of HCHO in the forest regions without obvious anthropogenic impact (Palmer et al., 2003), we used HCHO as the proxy of isoprene to validate the interannual variability of isoprene estimates.

2.5 Scenarios and Analysis Method

We designed four scenarios (S1-S4) to investigate the impact of land cover change and climatic conditions on BVOC emission. The configurations of the four scenarios are shown in Table 1, and S1 was considered as the standard or "full" scenario with both annually updated land cover parameters (LAIv and PFT) and meteorological conditions. S2 used the fixed meteorological conditions of the year 2001 and annually updated land cover parameters to investigate solely the impact of the ecosystem and land cover variability on BVOC emission. S3 and S4 adopted the land cover conditions of the year 2001 and 2016 respectively with annually updated meteorological fields to characterize the effect of climate variability on BVOC emission and compare the difference in BVOC emission induced by vegetation change in China between 2001 to 2016.

The climatic variability can affect the growth of vegetation and then affect LAI values (Piao et al., 2015). In this study, the interaction between climate and ecosystem is not considered in the offline MEGAN model, which means that the meteorological conditions, e.g. precipitation, will not affect the LAI values. The LAI input for MEGAN model in this study was obtained from the remote sensed LAI products. Therefore, when the time of the meteorological condition is inconsistent with that of the LAI input, the indirect impact of meteorological conditions on BVOC emission through biomass and phenology were

neglected. We used the experiments with the inconsistent LAI and meteorological conditions to investigate the direct effect of climatic variability on BVOC emission.

The chemical species emissions estimated by MEGAN were grouped into four major categories including isoprene, monoterpene, sesquiterpene and other VOCs since the terpenoids account for the majority of

5 total BVOC emission and have known impacts on atmospheric oxidants and SOA (Wang et al., 2011). The trend analysis in this study was done following the Theil-Sen trend estimation method and the results were tested by the Mann-Kendall non-parametric trend test, and the corresponding results in this study were calculated using the trend_manken (https://www.ncl.ucar.edu/Document/Functions/Built-in/trend_manken.shtml) function of the NCAR Command Language (NCL, https://www.ncl.ucar.edu/).

10 **3 Results and Discussion**

3.1 The Variability of BVOC Emission in China During 2001-2016

As shown in Table 2, the average annual emission during 2001-2016 of isoprene, monoterpene, sesquiterpene and other VOCs estimated from S1 are 7.56 (±0.74), 1.37 (±0.12), 0.16 (±0.02) and 6.73 (±0.46) Tg, respectively. Isoprene is the dominant species and accounts for about half of the total BVOC

15 emission in China. S1 is the standard scenario that includes both annually updated meteorological fields and vegetation conditions. In comparison with previous studies (Table 3), our estimation of isoprene emission is very close to the results by Stavrakou et al. (2014) and Tie et al. (2006) while our estimation of monoterpene emission is considerably (57 to 72%) lower than other estimations. Multiple factors including interannual variations, horizontal resolution, meteorological and land cover inputs can lead to

20 the discrepancy of these estimations.

The total estimated BVOC emission has a statistically significant increasing trend with rates of 1.09 and 1.19% yr-1 for the S1 and S2 scenarios (d in Figure 2), respectively. The increasing rate of isoprene, monoterpene and sesquiterpene are 1.35, 1.25 and 1.43% yr-1 respectively for the S1 scenario. In comparison, the increasing rates of these species in the S2 scenario are higher than those in the S1 scenario

25 with 1.58, 1.51 and 1.61 % yr-1 for isoprene, monoterpene and sesquiterpene despite the direct impact of meteorological conditions. Although the S1 scenario considers the impact of annual meteorological variability, the BVOC emission is still in a significant upward trend driven by the increasing forest area

and leaf mass. The lack of a significant trend of BVOC emission for both S3 and S4, with fixed landcover and annually updated meteorological conditions, demonstrates that meteorology was not an important driver of BVOC emission change in China during this period. Climatic conditions could affect the BVOC emission indirectly by affecting the growth of vegetation and controlling BVOC emission (Peñuelas et

5 al., 2009), which is not considered in the model used in this study. Therefore, our results only represent the direct impact of meteorological conditions on BVOC emission.

3.2 The Impact of Land Cover Changes and Meteorological Variability

The surface vegetation change had a significant influence on BVOC emissions in China during 2001-2016. In S2, the interannual variability of total BVOC emission is primarily determined by the surface

10 vegetation change resulting in a nearly linear increasing trend of BVOC emission. The average annual emission of total BVOC during the later eight years (2009-2016) is 8.50% (1.29 Tg) higher than that during the previous eight years (2001-2008). The average annual emissions of isoprene, monoterpene and sesquiterpene during the previous eight years are 11.3% (0.79 Tg), 11.9% (0.15 Tg) and 11.5% (0.02 Tg) higher than those during next eight years, respectively. The comparison of S3 and S4 results further

15 demonstrate the importance of vegetation development on BVOC emission considering the interannual variability of meteorological conditions. S3 and S4 adopted the same annually updated meteorological field but the fixed land cover information of the year 2001 and 2016, respectively. The fluctuation of meteorological factors leads to an interannual fluctuation of BVOC emission in S3 and S4, but the increase of vegetation cover rate in 2016 results in BVOC emissions that are much higher than in 2001

20 under the same meteorological conditions. As presented in Table 2, the average total BVOC emissions are 14.2 (±0.70) and 17.6 (±0.89) Tg in S3 and S4, respectively, and the total BVOC emission in S4 is 23.5% (3.35 Tg) higher than that in S3. The emissions of isoprene, monoterpene and sesquiterpene with the land cover information of the year 2016 are 29.9% (2.00 Tg), 27.4% (0.34 Tg) and 26.7% (0.04 Tg) higher than those estimated based on the land cover information of the year 2001, respectively.

25 The comparison among different scenarios indicates that the land cover change has comparative impact on annual BVOC variability with the meteorological fluctuation. The coefficient of variance (CV) of total BVOC emission in S3 and S4 is about 5% during 2001-2016, which is due to the interannual

meteorological variability. Furthermore, as shown in Figure 2, the largest discrepancy in total BVOC emission in S3 and S4 appears between the year 2014 and 2016, with the total BVOC emission in the year 2016 being 21.1 % and 22.5 % higher than that of the year 2014 in S3 and S4, respectively. In general, the interannual variability of meteorological conditions leads to ~20% difference in BVOC emission

5 during our study period. In contrast, the CV of total BVOC in S2 is 5.74%, which is close to that of 5% in S3 and S4, showing that interannual variability is dominated by meteorology even though the trend is dominated by landcover. Moreover, the largest discrepancy of total BVOC in S2 (23.9%) occurred between the year 2002 and 2016 and is very close to that estimated solely for meteorological conditions. However, as mentioned above, the comparison here only considered the direct impact of meteorological

10 conditions, and the meteorological conditions also can affect the growing process and phenology which can influence BVOC emission indirectly (Peñuelas et al., 2009). Considering the direct and indirect impact of climatic conditions as well as land cover change, the CV of total BVOC in the "full" scenario S1 is 8.15%, which is higher than the other scenarios. The highest and lowest total BVOC emission in S1 are in year 2016 and 2010, respectively, with 2016 being 34.60% (5.00 Tg) higher than 2010. These

15 results show that both landcover and meteorology can individually contribute ~20%, and together over 30%, to the estimated annual variability in China BVOC emissions within this 16-year time period.

3.3 The Regional Variability of BVOC Emission in China

The hotspots of BVOC emission are mainly located in the northeast, central and south of China where the forest is widely distributed and the climate is warm and favorable for emitting BVOC as shown in Figure

20 3. The Changbai Mountains, Qinling Mountains, the southeast and southwest China forest regions, southeast Tibet and Taiwan are the regions with highest BVOC emission in 2001, which is broadly consistent with the previous estimations (Tie et al., 2006; Li et al., 2013).

The spatial distributions of statistically significant (p>0.9) changing trends in S1-S4 are also presented for individual categories in Figure 3. In general, the spatial distributions of trends of different species in

25 S1 and S2 are highly consistent since the vegetation development is the main driver of the increasing trend of BVOC emission. A strong positive trend is found in the Qinling Mountains, southern China (Guangdong and Guangxi provinces) and southwestern China (Yunnan province), on the other hand, the

strong negative trend is found at the boundary of Jiangxi and Hunan provinces. While a positive increasing trend induced by meteorology is also found in Tibet, western Sichuan and southeastern Yunnan province in S3 and S4, and it is clear that most of the trend hotspots in S2 do not overlap with those in S3 and S4, which further indicates that the vegetation development is the main driver of BVOC increasing trend in

5   S1, the "full" scenario, rather than meteorological conditions.

We chose three main regions to analyze the hotspots of changing BVOC trend driving by the vegetation change, as shown in Figure 3r: Qinling Mountains (30-35N, 104-112E), the boundary region of Jiangxi and Hunan provinces (24.5-29N, 112-115E) and southern China, mainly Guangxi and Guangdong provinces (21-24.5N, 106-117E). The annual changes of vegetation conditions (PFT and LAI) and

10   emission rate in these three regions are presented in Figure 4. The (a), (b) and (c) in Figure 4 illustrate the vegetation and BVOC emission change in Qinling Mountains, southern China and the boundary of Jiangxi and Hunan provinces, respectively.

As shown in Figure 3, the Qinling Mountains and southern China are the regions with high BVOC emission as well as a significant increasing trend of BVOC emission. The mean emission flux in the

15   Qinling Mountains of approximately 3.91 g m-2 yr-1 in 2001 increased by 61.9 and 40.4 % to 6.33 and 5.49 g m-2 yr-1 in S1 and S2 in 2016, respectively. Southern China also shows a strong enhancement of BVOC emission. The mean emission rate is about 4.11 g m-2 yr-1 in 2001 and increased by 67.6 and 47.4 % to 6.89 and 6.06 g m-2 yr-1 in S1 and S2 respectively in 2016. Interestingly, the vegetation change patterns are notably different in the two regions. We grouped the PFTs used to estimate BVOC emission

20   into three main categories, broadleaf tree, needleleaf tree and other vegetations. As shown in Figure 4a, the total vegetation cover fraction increased by 0.105, from 0.578 in 2001 to 0.683 in 2016, in the Qinling Mountains region. All three of the PFTs categories contributed to the increasing vegetation cover trend in the Qinling Mountains from 2001 to 2016 including 0.207 to 0.262 (0.055 increase) for broadleaf trees, 0.004 to 0.007 (0.003 increase) for needleleaf trees and 0.366 to 0.414 (.048 increase) for other vegetation.

25   The percent contribution of each PFT category to the total vegetation cover fraction increase was about 52% for broadleaf trees, 3% for needleleaf trees and 45% for other vegetation. In contrast, there is only a small (0.017) change in total vegetation cover fraction in Southern China where the total vegetation cover fraction increased from 0.225 in 2001 to 0.242 in 2016. The major vegetation change in this region, as

shown in Figure 4b, is the deforestation that leads to the decrease of broadleaf forest and the increase of other vegetation, primarily cropland, from 2001 to 2005 followed by the decline in other vegetation since 2006 along with the increase in broadleaf tree cover fraction since 2007. The cover fractions of broadleaf tree, needleleaf tree and other vegetation in southern China changed from 0.127, 0.0001 and 0.097 in

5 2001 to 0.179, 0.0002 and 0.0626 in 2016, respectively. As a result, the 0.0522 broadleaf tree cover fraction plus the small 0.0001 needleleaf tree cover fraction increase was partially offset by the 0.0353 vegetation cover fraction decrease of other vegetation. Since the broadleaf trees tend to have a higher emission potential than grass or crop (Guenther et al., 2012), the transformation of land cover from grass or crop to broadleaf tree is expected to enhance the emission of BVOC by increasing the landscape

10 average emission factor. BVOC emission shows a statistically significant negative trend at the boundary region of Hunan and Jiangxi province in (Figure 3). As shown in Figure 4c, there was a BVOC emission decreasing trend from 2001 to 2010 and an increasing trend from 2011 to 2016 as a result of changes in the broadleaf tree cover fraction. As mentioned above, broadleaf tree has a relatively higher BVOC emission potential compared to other PFTs, therefore, the change of broadleaf tree cover rate induced by

15 anthropogenic activities is expected to affect local BVOC emission as shown in Figure 4. Compared to the lowest point of 0.177 in 2010, the cover fraction of broadleaf tree in this region recovers to 0.21 in 2016, which is still lower than the 2001 value of 0.224. In S2, the average emission rate of BVOC in this region in 2016 is 5.32 g m-2 yr-1 and is 2.91% lower than that in 2001 of 5.48 g m-2 yr-1. The lowest average emission rate during the study period appears in 2010 because of the lowest cover fraction of

20 broadleaf trees. However, in S1 with the impact of meteorological variability, the average emission rate in 2016 is 5.89 g m-2 yr-1. This is 7.48% higher than the average emission rate in 2001 of 5.48 g m-2 yr-1, but the lowest average emission rate of 4.49 g m-2 yr-1 is still in 2010. In general, it is clear that land cover change is a dominate factor impacting the interannual variability of BVOC emission on a decadal scale in regions undergoing rapid landcover change as has been suggested by previous studies (Unger,

25 2014; Chen et al., 2018).

The estimated increase of BVOC in regions like the Qinling Mountains and southern China are expected to affect regional air quality. For the Qinling Mountains and surrounding areas, as estimated by Li et al. (2018) using the WRF-chem model, the average contribution of BVOC to O$_3$ could reach 16.8 ppb for the

daily peak concentration and 8.2 ppb for the 24h concentration in the urban region of Xi'an, one of the biggest cities near the Qinling Mountains suffering poor air quality in recent years(Yang et al., 2019). For southern China, Situ et al. (2013) reported that BVOC emission could contribute an average 7.9 ppb surface peak O_3 concentration for the urban area in the Pearl River Delta region, and the contribution from

5   BVOC even reached 24.8 ppb over PRD in November. Since BVOC plays an important role in local air quality, the change of BVOC emission may have an even greater effect on the local ozone pollution. For instance, the simulation study by Li et al. (2018) also found that the urban region of Xi'an is VOC-limited because of the abundant NOx emission there. Therefore, the increase of BVOC emission in the Qinling Mountains would further favor the formation of O_3 in the urban region of Xi'an.

10   **3.4 Comparison of Estimates of Isoprene Emission and Satellite Derived Formaldehyde Column Concentration**

The lack of long-term in-situ observations of BVOC in China makes it difficult to validate the variability and trend estimation of BVOC emission in this study. However, since biogenic isoprene is the dominant precursor of formaldehyde in rural regions with minimal anthropogenic influence (Palmer et al., 2003), remotely sensed HCHO observation can used as a proxy of isoprene emission to assess the interannual

15   variability of isoprene emission. The OMI HCHO VC product from 2005-2016 developed by BIRA-IASB (De Smedt et al., 2015) was used in this study, and we compared the summer (June-August) average HCHO VC records with the summer-average isoprene emission estimated in our study to evaluate our estimation of interannual variability of isoprene emission.

The average growing season LAI during 2005-2016 presented in Figure 5a indicates the spatial

20   distribution of vegetation in China. However, the spatial pattern of estimated isoprene emission (Figure 5b) differs from the spatial distribution of vegetation because of the variability of emission potentials among different PFTs in the MEGAN model as well as the climatic conditions. The spatial pattern of average summertime HCHO VC observed by the OMI sensor during 2005-2016 is also presented in Figure 5c. The highest summer HCHO concentrations in the US are mainly distributed in rural forest

25   regions dominated by biogenic emission (Palmer et al., 2003), while the highest summer HCHO concentrations in China are mainly distributed in developed regions like North China Plain where HCHO

concentration is dominated by anthropogenic sources. There is a moderate HCHO VC of about 6-10 ×10¹⁵ molec cm-2 in the vegetation dominated regions of China.

The grid level correlation coefficients between the average summer HCHO VC and isoprene emission estimated in our study are shown in Figure 5d, and the grids with statistically significant correlations (p>0.9, N=12) grids are marked with black dots. A positive correlation can be found in the northeast, central and south of China where there are relatively high vegetation cover rates and low anthropogenic influence. In contrast, there's almost no statistically significant correlation in the high HCHO VC regions like the North China Plain which is dominated by anthropogenic emissions. In addition, there is also no significant correlations between isoprene emission and HCHO VC in regions like the Pearl River Delta where HCHO concentration is controlled by both biogenic and anthropogenic sources. However, the distribution of statistically significant positive correlated points is not completely consistent with the vegetation distribution indicated by LAI because of the absence of consideration of physical and chemical processes, including transportation, diffusion, and chemical reactions. The grids with significant correlation are mostly distrusted in or near rural regions with high vegetation biomass indicating that our estimations can represent the annual variation of isoprene emission.

The increasing trends of isoprene and HCHO VC during 2005-2016 are presented in (e) and (f) of Figure 5, and the statistically significant (p>0.9) grids are marked with black dots. The increasing trend pattern of isoprene emission during 2005-2016 is basically consistent with that during 2001-2016, which has been described in the previous section, and it is clear that central and southern China are the regions with the greatest increasing trend (> 0.06 g m-2 yr-1). For HCHO, developed regions such as the North China Plain have an increasing trend because of the increase of human activities (Smedt et al., 2010), there is also an obvious increasing trend of HCHO VC in the developed Yunnan and Guangxi provinces in the south of China. Moreover, these regions, especially Guangxi province also show a statistically significant positive correlation between isoprene emission and HCHO VC as presented in Figure 5d. This indicates that biogenic emissions might be the main driver of the increased HCHO in Guangxi province.

3.5 Comparison of BVOC Emission with Anthropogenic Emission in China.

China has initiated a series of pollution control policies in recent years (Zheng et al., 2018; Ma et al., 2019) and achieved success in controlling some air pollutants, especially PM2.5 (Ma et al., 2019; Yu et al., 2019; Xu et al., 2019). However, the ozone pollution is still severe in China especially the mega-city
areas (Li et al., 2019; Xu et al., 2019). It is widely known that NOx and VOC are the precursors of ground level ozone pollution (Seinfeld and Pandis, 2012). NOx emission in China increased from 2010 to 2012 and then declined rapidly since 2013 because of the emission control policies, and the national-level NOx emission is about 22.50 Tg in 2016 and is ~15 % lower than that in 2010 (Zheng et al., 2018). On the other hand, as shown in Figure 6, the average anthropogenic volatile organic compounds (AVOC)
emission during 2010-2016 was about 27.9 Tg in China (Zheng et al., 2018), which is ~70% higher than the average emission of BVOC during the same period investigated by this study. It is clear that the anthropogenic source currently dominates non-methane volatile organic compound (NMVOC) emissions in China. In addition, the spatial distribution of remotely sensed HCHO VC (Figure 5) also indicates the dominant role of anthropogenic NMVOC emission.

The urban areas in China are generally in the VOC-limited condition and decreasing/increasing local NOx/VOC emission would correspondingly promote the formation of ozone (Tang et al., 2010; Li et al., 2018; Li et al., 2019). Both AVOC and BVOC show the increasing trend since 2010, as shown in Figure 6, with an increase of 9.7% for AVOC and 34.6% for BVOC from 2010 to 2016, respectively. Combined with the decreasing trend of NOx emission, the overall changes of precursors are expected to make it
more difficult to control ozone pollution. In addition, there are multiple studies pointing out the interactions between anthropogenic emission and biogenic emission on ozone pollution in mega cities including Beijing (Pang et al., 2009;Shao et al., 2009), Shanghai (Geng et al., 2011), Guangzhou (Situ et al., 2013) and Xi'an (Li et al., 2018). The current trends in biogenic as well as anthropogenic emissions suggest that biogenic emissions will play an even more important role in future air pollution in China.

4. Conclusion

Satellite observations have shown that China has led the global greening trend in recent decades (Chen et al., 2019). In this study, we investigated the impact of this greening trend on BVOC emission in China

during 2001 to 2016. We used the long-term satellite vegetation products as inputs for the MEGAN model. According to the model estimations, the total BVOC emission in China had a significant increasing trend of 1.09% yr-1 during 2001-2016, and main BVOC classes of isoprene, monoterpene and sesquiterpene all had increasing trends of 1.35 % yr-1, 1.25 % yr-1 and 1.43 % yr-1. The comparison among different scenarios showed that vegetation changes resulting from land cover management is the main driver of BVOC emission change in China. Climate variability contributed significantly to interannual variations but not the long-term trend.

On regional scales, there are strong increasing trends in the Qinling Mountains, southern China (Guangdong and Guangxi provinces) and southwestern China, while a strong negative trend was found at the boundary of Jiangxi and Hunan provinces. In the standard scenario, that considers both land cover and climate, the BVOC emission of year 2016 is 61.89% and 67.64% higher than that in 2001 in the Qinling Mountains and southern China, respectively; furthermore, the land cover change alone could lead to 40.40% and 47.44% increase of BVOC emission in the Qinling Mountains and southern China, respectively. Moreover, the vegetation change patterns are different in the two regions. In the Qinling Mountains, the total vegetation cover rate obviously increased from 0.578 in 2001 to 0.683 in 2016, and all three main PFT categories, i.e. broadleaf trees, needleleaf trees and other vegetations, increased during 2001-2016.

In contrast there the total vegetation cover fraction only increased from 0.225 in 2001 to 0.242 in 2016 southern China, but this was due to the replacement of low BVOC emission potential PFTs, crops or grass, with forests that have much higher emission potential. There is also a significantly negative trend at the boundary region of Hunan and Jiangxi provinces (Figure 3) induced by deforestation during 2001-2010. However, the BVOC emission there has been in a increasing trend since 2011 with the recovery of the broadleaf tree forest.

We used the long-term record of satellite HCHO VC from the OMI sensor to asses our estimation of isoprene emission in China during 2005-2016. The results indicated statistically significant positive correlation coefficients between the isoprene emission estimate and satellite HCHO VC in summer over the regions with high vegetation cover fraction including the northeast, central and southern China. In addition, isoprene emission and HCHO VC both had a statistically significant increasing trend in the

south of China, mainly Guangxi Province, where there was a statistically significant positive correlation supporting the estimated variability of BVOC emission in China.

The increase of BVOC reported by this study is expected to lead to a more complex situation for making the policies for controlling ozone pollution in China. The recent pollution control policies in China have 5 effectively initiated the control of PM2.5 pollution, but the ozone pollution is still severe especially in urban areas (Ma et al., 2019; Yu et al., 2019; Xu et al., 2019; Li et al., 2019). Although anthropogenic emission is still the dominant source of NMVOC in China and is ~70 % higher than the average biogenic emission in China, the BVOC still makes an important contribution to ozone pollution in mega cities including Beijing (Pang et al., 2009;Shao et al., 2009), Shang Hai (Geng et al., 2011), Guang Zhou (Situ 10 et al., 2013) and Xi'an (Li et al., 2018) and may further increase in importance considering the continuing greening trend over China in the future.

Author Contribution

QW, LW and HW planned and organized the project. HW, JF and QX prepared the input datasets. HW modelled and analyzed the data. HW and QW wrote the manuscript. HW, AG and QW revised the 15 manuscript. AG, XY, LN, XT, JL, JF and HC reviewed and provided key comments on the paper.

Data Availability

The source code of MEGAN v2.1 is available at https://bai.ess.uci.edu/. The MODIS MCD12C1 land cover product Version 6 and MODIS MCD15A2 LAI Version 6 and MODIS MOD44B VCF Version 6 datasets are available on the website of the Land Processes Distributed Active Archive Center (LP DAAC) 20 at https://lpdaac.usgs.gov/dataset_discovery/modis/modis_products_table. The version 14 Level 3 OMI HCHO VC product were downloaded from the website of Tropospheric Emission Monitoring Internet Service (TEMIS) at http://h2co.aeronomy.be.

Competing Interests

The authors declare no competing financial interest.

Acknowledgements

The National Key R&D Program of China (2017YFC0209805 and 2016YFB0200800), the National Natural Science Foundation of China (41305121) and the Fundamental Research Funds for the Central Universities funded this work.

5 **References**

Arneth, A., Niinemets, Ü., Pressley, S., Bäck, J., Hari, P., Karl, T., Noe, S., Prentice, I., Serça, D., and Hickler, T.: Process-based estimates of terrestrial ecosystem isoprene emissions: incorporating the effects of a direct CO_2-isoprene interaction, Atmospheric Chemistry and Physics, 7, 31-53, 2007.

Berrisford, P., Dee, D. P., Poli, P., Brugge, R., Mark, F., Manuel, F., Kållberg, P. W., Kobayashi, S., Uppala, S., and Adrian,
10 S.: The ERA-Interim archive Version 2.0, ECMWF, Shinfield Park, Reading, 2011.

Bonan Gordon, B., Levis, S., Kergoat, L., and Oleson Keith, W.: Landscapes as patches of plant functional types: An integrating concept for climate and ecosystem models, Global Biogeochemical Cycles, 16, 5-1-5-23, 10.1029/2000GB001360, 2002.

Bryan, B. A., Gao, L., Ye, Y., Sun, X., Connor, J. D., Crossman, N. D., Stafford-Smith, M., Wu, J., He, C., Yu, D., Liu, Z.,
15 Li, A., Huang, Q., Ren, H., Deng, X., Zheng, H., Niu, J., Han, G., and Hou, X.: China's response to a national land-system sustainability emergency, Nature, 559, 193-204, 10.1038/s41586-018-0280-2, 2018.

Chen, C., Park, T., Wang, X., Piao, S., Xu, B., Chaturvedi, R. K., Fuchs, R., Brovkin, V., Ciais, P., Fensholt, R., Tømmervik, H., Bala, G., Zhu, Z., Nemani, R. R., and Myneni, R. B.: China and India lead in greening of the world through land-use management, Nature Sustainability, 2, 122-129, 10.1038/s41893-019-0220-7, 2019.

20 Chen, W. H., Guenther, A. B., Wang, X. M., Chen, Y. H., Gu, D. S., Chang, M., Zhou, S. Z., Wu, L. L., and Zhang, Y. Q.: Regional to Global Biogenic Isoprene Emission Responses to Changes in Vegetation From 2000 to 2015, Journal of Geophysical Research: Atmospheres, 123, 3757-3771, 10.1002/2017JD027934, 2018.

Claeys, M., Graham, B., Vas, G., Wang, W., Vermeylen, R., Pashynska, V., Cafmeyer, J., Guyon, P., Andreae, M. O., and Artaxo, P.: Formation of secondary organic aerosols through photooxidation of isoprene, Science, 303, 1173-1176, 2004.

25 De Smedt, I., Van Roozendael, M., Stavrakou, T., Müller, J. F., Lerot, C., Theys, N., Valks, P., Hao, N., and van der A, R.: Improved retrieval of global tropospheric formaldehyde columns from GOME-2/MetOp-A addressing noise reduction and instrumental degradation issues, Atmos. Meas. Tech., 5, 2933-2949, 10.5194/amt-5-2933-2012, 2012.

De Smedt, I., Stavrakou, T., Hendrick, F., Danckaert, T., Vlemmix, T., Pinardi, G., Theys, N., Lerot, C., Gielen, C., Vigouroux, C., Hermans, C., Fayt, C., Veefkind, P., Müller, J. F., and Van Roozendael, M.: Diurnal, seasonal and long-term variations of
30 global formaldehyde columns inferred from combined OMI and GOME-2 observations, Atmos. Chem. Phys., 15, 12519-12545, 10.5194/acp-15-12519-2015, 2015.

Dobber, M., Kleipool, Q., Dirksen, R., Levelt, P., Jaross, G., Taylor, S., Kelly, T., Flynn, L., Leppelmeier, G., and Rozemeijer, N.: Validation of Ozone Monitoring Instrument level 1b data products, Journal of Geophysical Research: Atmospheres, 113, 10.1029/2007JD008665, 2008.

Fu, Y., and Liao, H.: Simulation of the interannual variations of biogenic emissions of volatile organic compounds in China: Impacts on tropospheric ozone and secondary organic aerosol, Atmospheric Environment, 59, 170-185, https://doi.org/10.1016/j.atmosenv.2012.05.053, 2012.

Geng, F., Tie, X., Guenther, A., Li, G., Cao, J., and Harley, P.: Effect of isoprene emissions from major forests on ozone formation in the city of Shanghai, China, Atmospheric Chemistry and Physics, 11, 10449-10459, 10.5194/acp-11-10449-2011, 2011.

Guenther, A., Hewitt, C. N., Erickson, D., Fall, R., Geron, C., Graedel, T., Harley, P., Klinger, L., Lerdau, M., McKay, W. A., Pierce, T., Scholes, B., Steinbrecher, R., Tallamraju, R., Taylor, J., and Zimmerman, P.: A global model of natural volatile organic compound emissions, Journal of Geophysical Research, 100, 8873, 10.1029/94jd02950, 1995.

Guenther, A., Karl, T., Harley, P., Wiedinmyer, C., Palmer, P., and Geron, C.: Estimates of global terrestrial isoprene emissions using MEGAN (Model of Emissions of Gases and Aerosols from Nature), Atmos. Chem. Phys, 6, 3181-3210, 2006.

Guenther, A. B., Monson, R. K., and Fall, R.: Isoprene and monoterpene emission rate variability: Observations with eucalyptus and emission rate algorithm development, Journal of Geophysical Research: Atmospheres, 96, 10799-10808, 10.1029/91JD00960, 1991.

Guenther, A. B., Zimmerman, P. R., Harley, P. C., Monson, R. K., and Fall, R.: Isoprene and monoterpene emission rate variability: Model evaluations and sensitivity analyses, Journal of Geophysical Research: Atmospheres, 98, 12609-12617, doi:10.1029/93JD00527, 1993.

Guenther, A. B., Jiang, X., Heald, C. L., Sakulyanontvittaya, T., Duhl, T., Emmons, L. K., and Wang, X.: The Model of Emissions of Gases and Aerosols from Nature version 2.1 (MEGAN2.1): an extended and updated framework for modeling biogenic emissions, Geoscientific Model Development, 5, 1471-1492, 10.5194/gmd-5-1471-2012, 2012.

Guenther, C.: Estimates of global terrestrial isoprene emissions using MEGAN (Model of Emissions of Gases and Aerosols from Nature), Atmospheric Chemistry and Physics, 6, 2006.

Heald, C. L., Wilkinson, M. J., Monson, R. K., Alo, C. A., Wang, G., and Guenther, A.: Response of isoprene emission to ambient CO2 changes and implications for global budgets, Global Change Biology, 15, 1127-1140, doi:10.1111/j.1365-2486.2008.01802.x, 2009.

Jin, X., and Holloway, T.: Spatial and temporal variability of ozone sensitivity over China observed from the Ozone Monitoring Instrument, Journal of Geophysical Research: Atmospheres, 120, 7229-7246, doi:10.1002/2015JD023250, 2015.

Kaiser, J., Jacob, D. J., Zhu, L., Travis, K. R., Fisher, J. A., González Abad, G., . . . Wisthaler, A. (2018). High-resolution inversion of OMI formaldehyde columns to quantify isoprene emission on ecosystem-relevant scales: application to the southeast US. Atmos. Chem. Phys., 18(8), 5483-5497. doi:10.5194/acp-18-5483-2018

Kavouras, I. G., Mihalopoulos, N., and Stephanou, E. G.: Formation of atmospheric particles from organic acids produced by forests, Nature, 395, 683-686, 1998.

Klinger, L. F., Li, Q. J., Guenther, A. B., Greenberg, J. P., Baker, B., and Bai, J. H.: Assessment of volatile organic compound emissions from ecosystems of China, Journal of Geophysical Research: Atmospheres, 107, ACH 16-11-ACH 16-21, 10.1029/2001jd001076, 2002.

Lathière, J., Hewitt, C. N., and Beerling, D. J.: Sensitivity of isoprene emissions from the terrestrial biosphere to 20th century changes in atmospheric CO_2 concentration, climate, and land use, Global Biogeochemical Cycles, 24, 10.1029/2009GB003548, 2010.

Lawrence, D. M., Oleson, K. W., Flanner, M. G., Thornton, P. E., Swenson, S. C., Lawrence, P. J., Zeng, X., Yang, Z. L., Levis, S., and Sakaguchi, K.: Parameterization improvements and functional and structural advances in Version 4 of the Community Land Model, Journal of Advances in Modeling Earth Systems, 3, 365-375, 2011.

Li, K., Jacob, D. J., Liao, H., Shen, L., Zhang, Q., and Bates, K. H.: Anthropogenic drivers of 2013–2017 trends in summer surface ozone in China, Proceedings of the National Academy of Sciences, 116, 422, 10.1073/pnas.1812168116, 2019.

Li, L. Y., Chen, Y., and Xie, S. D.: Spatio-temporal variation of biogenic volatile organic compounds emissions in China, Environmental Pollution, 182, 157-168, https://doi.org/10.1016/j.envpol.2013.06.042, 2013.

Li, L. Y., and Xie, S. D.: Historical variations of biogenic volatile organic compound emission inventories in China, 1981–2003, Atmospheric Environment, 95, 185-196, https://doi.org/10.1016/j.atmosenv.2014.06.033, 2014.

Li, N., He, Q., Greenberg, J., Guenther, A., Li, J., Cao, J., Wang, J., Liao, H., Wang, Q., and Zhang, Q.: Impacts of biogenic and anthropogenic emissions on summertime ozone formation in the Guanzhong Basin, China, Atmos. Chem. Phys., 18, 7489-7507, 10.5194/acp-18-7489-2018, 2018.

Ma, Z., Liu, R., Liu, Y., and Bi, J.: Effects of air pollution control policies on PM2.5 pollution improvement in China from 2005 to 2017: a satellite-based perspective, Atmos. Chem. Phys., 19, 6861-6877, 10.5194/acp-19-6861-2019, 2019.

Marais, E. A., Jacob, D. J., Kurosu, T., Chance, K., Murphy, J., Reeves, C., Mills, G., Casadio, S., Millet, D., and Barkley, M. P.: Isoprene emissions in Africa inferred from OMI observations of formaldehyde columns, Atmospheric Chemistry and Physics, 12, 6219-6235, 2012.

Müller, J. F., Stavrakou, T., Wallens, S., De Smedt, I., Van Roozendael, M., Potosnak, M. J., . . . Guenther, A. B. (2008). Global isoprene emissions estimated using MEGAN, ECMWF analyses and a detailed canopy environment model. Atmos. Chem. Phys., 8(5), 1329-1341. doi:10.5194/acp-8-1329-2008

Palmer, P. I., Jacob, D. J., Fiore, A. M., Martin, R. V., Chance, K., and Kurosu, T. P.: Mapping isoprene emissions over North America using formaldehyde column observations from space, Journal of Geophysical Research: Atmospheres, 108, n/a-n/a, 10.1029/2002JD002153, 2003.

Pang, X., Mu, Y., Zhang, Y., Lee, X., and Yuan, J.: Contribution of isoprene to formaldehyde and ozone formation based on its oxidation products measurement in Beijing, China, Atmospheric Environment, 43, 2142-2147, http://dx.doi.org/10.1016/j.atmosenv.2009.01.022, 2009.

Penuelas, J., and Staudt, M.: BVOCs and global change, Trends Plant Sci, 15, 133-144, 10.1016/j.tplants.2009.12.005, 2010.

Peñuelas, J., Rutishauser, T., and Filella, I.: Phenology Feedbacks on Climate Change, Science, 324, 887, 10.1126/science.1173004, 2009.

Piao, S., Yin, G., Tan, J., Cheng, L., Huang, M., Li, Y., Liu, R., Mao, J., Myneni, R. B., Peng, S., Poulter, B., Shi, X., Xiao, Z., Zeng, N., Zeng, Z., and Wang, Y.: Detection and attribution of vegetation greening trend in China over the last 30 years, Global Change Biology, 21, 1601-1609, 10.1111/gcb.12795, 2015.

Sakulyanontvittaya, T., Duhl, T., Wiedinmyer, C., Helmig, D., Matsunaga, S., Potosnak, M., Milford, J., and Guenther, A.: Monoterpene and sesquiterpene emission estimates for the United States, Environmental science & technology, 42, 1623-1629, 2008.

Seinfeld, J. H., and Pandis, S. N.: Atmospheric Chemistry and Physics: From Air Pollution to Climate Change, 2nd Edition, 2012.

Shao, M., Lu, S., Liu, Y., Xie, X., Chang, C., Huang, S., and Chen, Z.: Volatile organic compounds measured in summer in Beijing and their role in ground-level ozone formation, Journal of Geophysical Research: Atmospheres, 114, 2009.

Sindelarova, K., Granier, C., Bouarar, I., Guenther, A., Tilmes, S., Stavrakou, T., Müller, J. F., Kuhn, U., Stefani, P., and Knorr, W.: Global data set of biogenic VOC emissions calculated by the MEGAN model over the last 30 years, Atmos. Chem. Phys., 14, 9317-9341, 10.5194/acp-14-9317-2014, 2014.

Situ, S., Guenther, A., Wang, X., Jiang, X., Turnipseed, A., Wu, Z., and Bai, J.: Impacts of seasonal and regional variability in biogenic VOC emissions on surface ozone in the Pearl River delta region, China, Atmospheric Chemistry and Physics, 13, 11803-11817, 2013.

Skamarock, W. C., Klemp, J. B., Dudhia, J., Gill, D. O., Barker, D. M., Duda, M. G., Huang, X.-y., Wang, W., and Powers, J. G.: A description of the advanced research WRF version 3, NCAR Technical Note NCAR/TN-475+STR, 2008.

Smedt, I. D., Stavrakou, T., Müller, J. F., R., J. v. d. A., and Roozendael, M. V.: Trend detection in satellite observations of formaldehyde tropospheric columns, Geophysical Research Letters, 37, L18808, 2010.

Stavrakou, T., Müller, J. F., Bauwens, M., De Smedt, I., Van Roozendael, M., Guenther, A., Wild, M., and Xia, X.: Isoprene emissions over Asia 1979-2012: impact of climate and land-use changes, Atmospheric Chemistry and Physics, 14, 4587-4605, 10.5194/acp-14-4587-2014, 2014.

Stavrakou, T., Müller, J. F., Bauwens, M., De Smedt, I., Van Roozendael, M., De Mazière, M., Vigouroux, C., Hendrick, F., George, M., Clerbaux, C., Coheur, P. F., and Guenther, A.: How consistent are top-down hydrocarbon emissions based on formaldehyde observations from GOME-2 and OMI?, Atmos. Chem. Phys., 15, 11861-11884, 10.5194/acp-15-11861-2015, 2015.

Stavrakou, T., Müller, J. F., Bauwens, M., Smedt, I., Roozendael, M., and Guenther, A.: Impact of Short-term Climate Variability on Volatile Organic Compounds Emissions Assessed Using OMI Satellite Formaldehyde Observations, Geophysical Research Letters, 0, 10.1029/2018GL078676, 2018.

Tang, X., Wang, Z., Zhu, J., Gbaguidi, A. E., Wu, Q., Li, J., and Zhu, T.: Sensitivity of ozone to precursor emissions in urban Beijing with a Monte Carlo scheme, Atmospheric Environment, 44, 3833-3842, http://dx.doi.org/10.1016/j.atmosenv.2010.06.026, 2010.

Tie, X., Li, G., Ying, Z., Guenther, A., and Madronich, S.: Biogenic emissions of isoprenoids and NO in China and comparison to anthropogenic emissions, Science of the total environment, 371, 238-251, 2006.

Unger, N.: Isoprene emission variability through the twentieth century, Journal of Geophysical Research: Atmospheres, 118, 13,606-613,613, 10.1002/2013JD020978, 2013.

Unger, N.: Human land-use-driven reduction of forest volatiles cools global climate, Nature Climate Change, 4, 907, 10.1038/nclimate2347 https://www.nature.com/articles/nclimate2347#supplementary-information, 2014.

Wang, H., Wu, Q., Liu, H., Wang, Y., Cheng, H., Wang, R., Wang, L., Xiao, H., and Yang, X.: Sensitivity of biogenic volatile organic compound emissions to leaf area index and land cover in Beijing, Atmos. Chem. Phys., 18, 9583-9596, 10.5194/acp-18-9583-2018, 2018.

Wang, X., Situ, S., Guenther, A., Chen, F. E. I., Wu, Z., Xia, B., and Wang, T.: Spatiotemporal variability of biogenic terpenoid emissions in Pearl River Delta, China, with high-resolution land-cover and meteorological data, Tellus B, 63, 241-254, 10.1111/j.1600-0889.2010.00523.x, 2011.

Xu, J., Tie, X., Gao, W., Lin, Y., and Fu, Q.: Measurement and model analyses of the ozone variation during 2006 to 2015 and its response to emission change in megacity Shanghai, China, Atmos. Chem. Phys., 19, 9017-9035, 10.5194/acp-19-9017-2019, 2019.

Yang, X., Wu, Q., Zhao, R., Cheng, H., He, H., Ma, Q., Wang, L., and Luo, H.: New method for evaluating winter air quality: PM2.5 assessment using Community Multi-Scale Air Quality Modeling (CMAQ) in Xi'an, Atmospheric Environment, 211, 18-28, https://doi.org/10.1016/j.atmosenv.2019.04.019, 2019.

Yu, M., Zhu, Y., Lin, C.-J., Wang, S., Xing, J., Jang, C., Huang, J., Huang, J., Jin, J., and Yu, L.: Effects of air pollution control measures on air quality improvement in Guangzhou, China, Journal of Environmental Management, 244, 127-137, https://doi.org/10.1016/j.jenvman.2019.05.046, 2019.

Zhang, Y., Peng, C., Li, W., Tian, L., Zhu, Q., Chen, H., Fang, X., Zhang, G., Liu, G., Mu, X., Li, Z., Li, S., Yang, Y., Wang, J., and Xiao, X.: Multiple afforestation programs accelerate the greenness in the 'Three North' region of China from 1982 to 2013, Ecological Indicators, 61, 404-412, https://doi.org/10.1016/j.ecolind.2015.09.041, 2016.

Zheng, B., Tong, D., Li, M., Liu, F., Hong, C., Geng, G., Li, H., Li, X., Peng, L., Qi, J., Yan, L., Zhang, Y., Zhao, H., Zheng, Y., He, K., and Zhang, Q.: Trends in China's anthropogenic emissions since 2010 as the consequence of clean air actions, Atmos. Chem. Phys., 18, 14095-14111, 10.5194/acp-18-14095-2018, 2018.

Zhu, L., Jacob, D. J., Keutsch, F. N., Mickley, L. J., Scheffe, R., Strum, M., González Abad, G., Chance, K., Yang, K., Rappenglück, B., Millet, D. B., Baasandorj, M., Jaeglé, L., and Shah, V.: Formaldehyde (HCHO) As a Hazardous Air Pollutant:

Mapping Surface Air Concentrations from Satellite and Inferring Cancer Risks in the United States, Environmental Science & Technology, 51, 5650-5657, 10.1021/acs.est.7b01356, 2017a.

Zhu, L., Mickley, L. J., Jacob, D. J., Marais, E. A., Sheng, J., Hu, L., Abad, G. G., and Chance, K.: Long-term (2005–2014) trends in formaldehyde (HCHO) columns across North America as seen by the OMI satellite instrument: Evidence of changing

5   emissions of volatile organic compounds, Geophysical Research Letters, 44, 7079-7086, 10.1002/2017GL073859, 2017b.

Table 1. Description of different scenarios used to estimate the BVOC emission.

	Land Cover	Meteorological conditions
S1	Annually updated	Annually updated
S2	Annually updated	Year 2001
S3	Year 2001	Annually updated
S4	Year 2016	Annually updated

Table 2. The mean annual China emission (Tg) of different species during 2001 to 2016. The scenarios S1 to S4 are described in Table 1.

	S1	S2	S3	S4
Isoprene	7.56 (±0.74)	7.40 (±0.56)	6.68 (±0.32)	8.68 (±0.45)
Monoterpenes	1.37 (±0.12)	1.35 (±0.10)	1.24 (±0.03)	1.58 (±0.05)
Sesquiterpenes	0.16 (±0.02)	0.16 (±0.01)	0.15 (±0.01)	0.19 (±0.01)
Other VOCs	6.73 (±0.46)	6.94 (±0.24)	6.16 (±0.36)	7.14 (±0.40)
Total BVOCs	15.82 (±1.29)	15.85 (±0.91)	14.23 (±0.70)	17.59 (±0.89)

Table 3. Comparison of isoprene and monoterpene emissions (Tg) in China with previous estimations.

Reference	Isoprene	Monoterpene	Study period	Method or Model
This study	7.56 (±0.74)	1.37 (±0.12)	2001-2016	MEGAN
Stavrakou et al. (2014)	7.17 (±0.30)	-	2007-2012	MEGAN-MOHYCAN
Li et al. (2013)	20.7	4.9	2003	MEGAN
Fu and Liao (2012)	10.87	3.21	2001-2006	GEOS-Chem-MEGAN

Tie et al. (2006)	7.7	3.16	2004	Guenther et al. (1993)
Klinger et al. (2002)	4.65	3.97	2000	Guenther et al. (1995)
Guenther et al. (1995)	17	4.87	1990	Guenther et al. (1995)
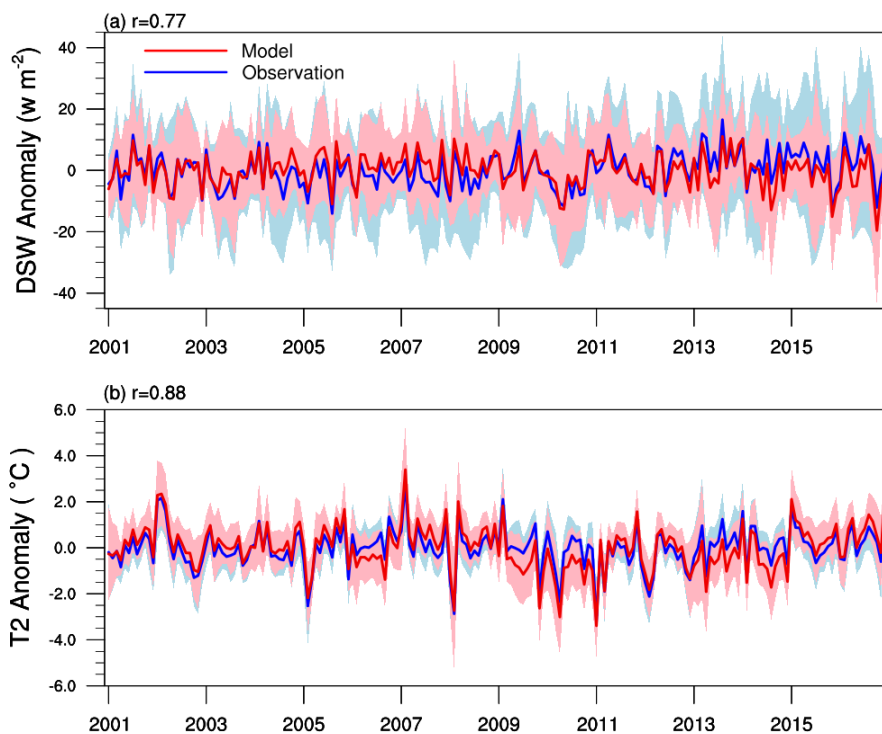
Figure 1. The comparison of monthly anomaly of downward shortwave (DSW) radiation (a) and 2-meter temperature (T2) (b) for model simulation and in-situ observation and the filled areas present the standard deviations among 98 sites for DSW and 697 sites for T2.
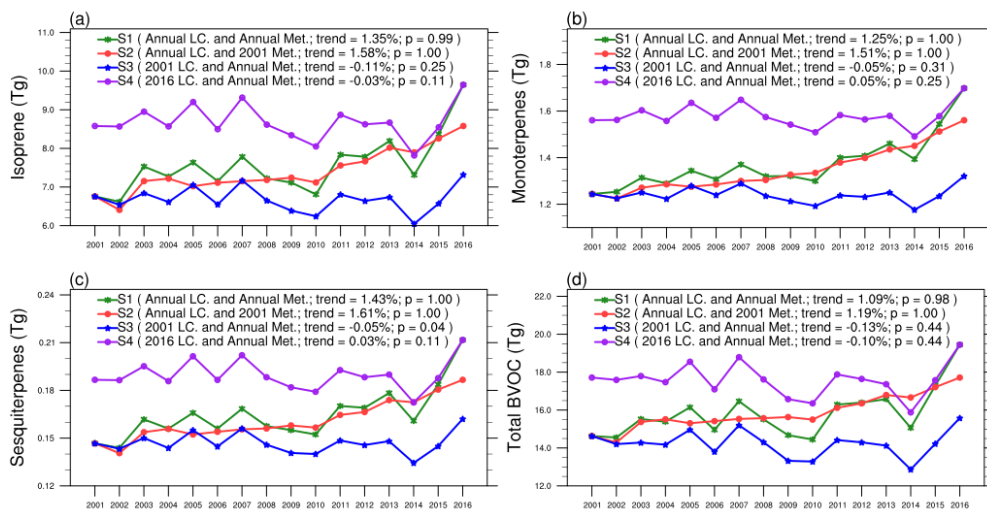
Figure 2. Annual BVOC emissions in China during 2001 to 2016 for four scenarios (S1-S4) described in Table 1. The increasing trends and the probabilities (p) using the Mann-Kendall test are shown in the legend.
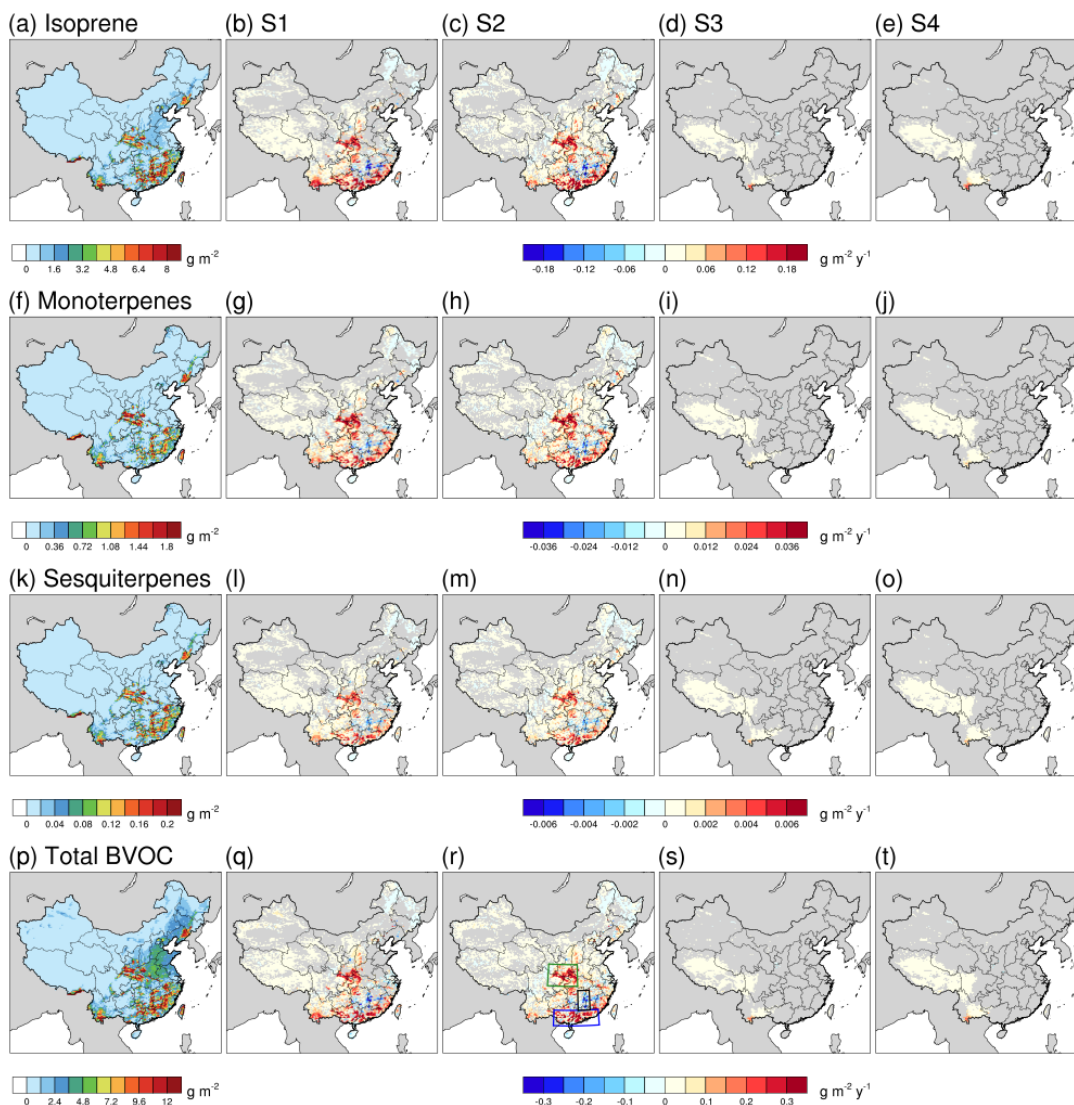
Figure 3. The horizontal distributions of isoprene, monoterpenes, sesquiterpenes and total BVOCs emissions of China in 2001 are showed in figure (a), (f), (k) and (p), respectively. The rest columns of figures present the changing trend of isoprene (b-e), monoterpenes (g-j), sesquiterpenes (l-o) and total BVOCs (q-t) in S1, S2, S3 and S4, respectively. The Mann-Kendall test were used to filter the grids where the p is lower than 0.9.
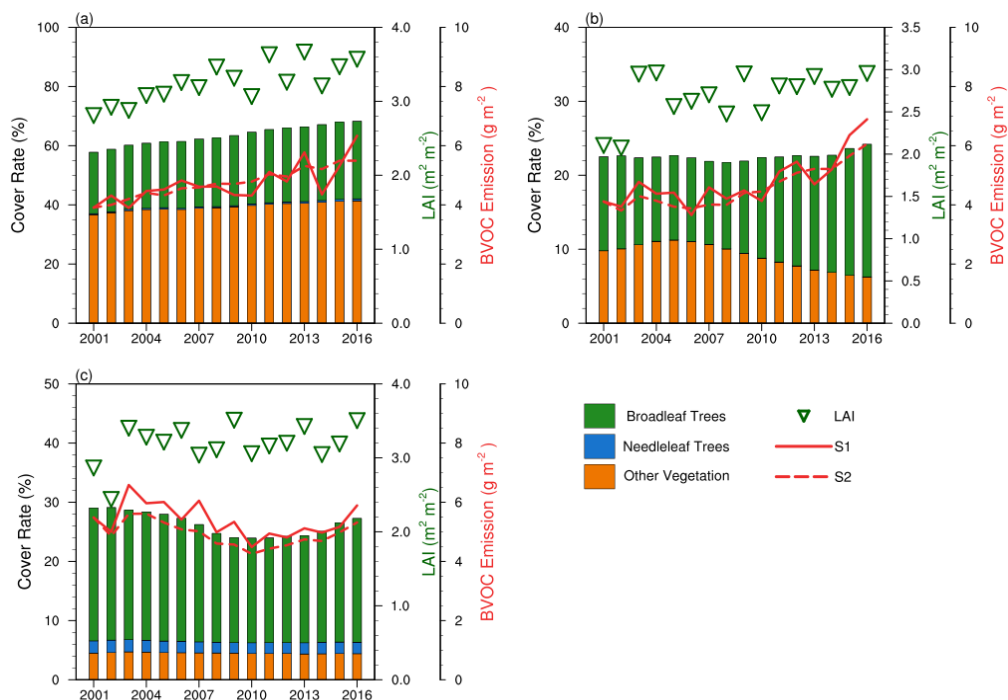
Figure 4. The annual changes of PFTs, emission rate of BVOC and LAI in (a) the Qinling Montains, (b) southern of China, and the (c) the Jiang Xi and Hu Nan province border. The solid and dashed line represents the mean emission flux rate of total BVOC in S1 and S2, respectively.
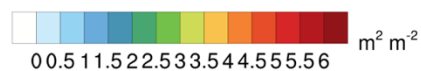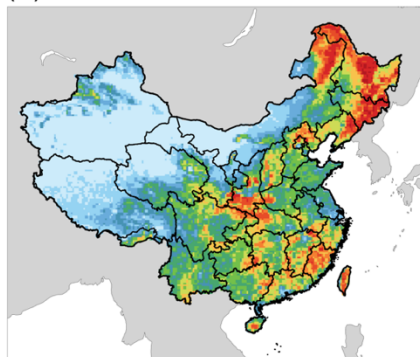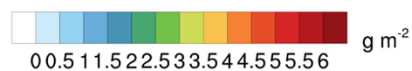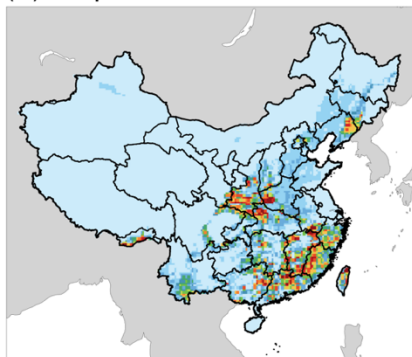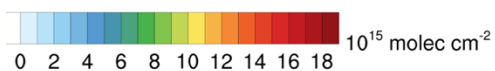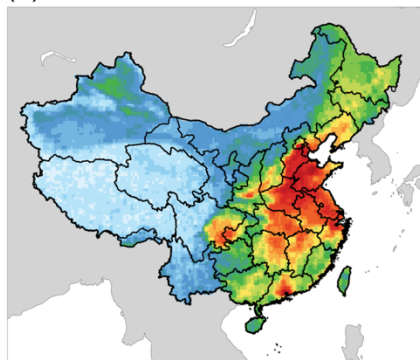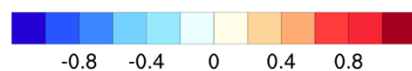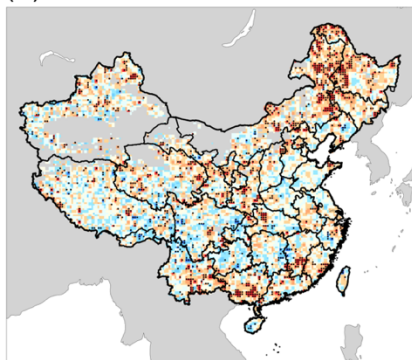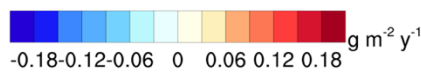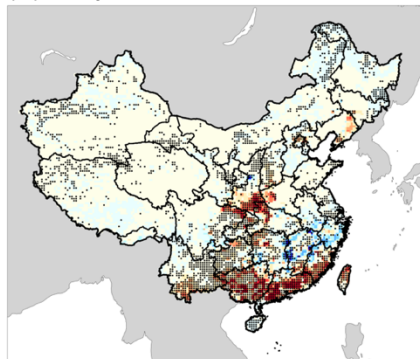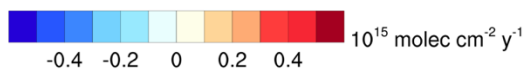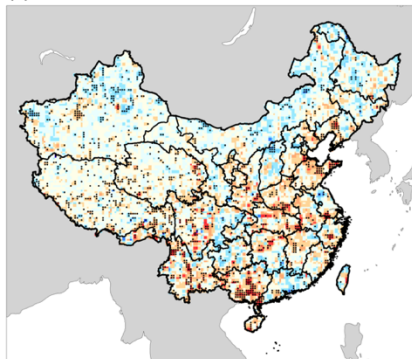
Figure 5. Comparison of estimated isoprene annual emission with the satellite derived tropospheric HCHO vertical column concentration by OMI during 2005-2016. (a), (b) and (c) illustrate the spatial distributions of growing-season mean LAI, isoprene emission and HCHO vertical columns (VC) by OMI respectively. (d) presents the spatial distribution of the correlation efficient between summertime isoprene emission and HCHO VC. (e) and (f) shows the increasing trend of isoprene and HCHO VC during 2005-2016.
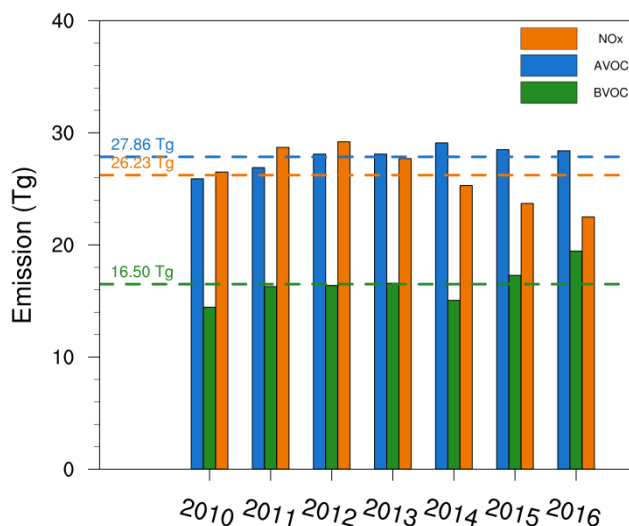
Figure 6. Comparison of BVOC emission with anthropogenic VOC (Zheng et al., 2018) and NOx emission in China during 2010-2016. The dashed lines represent the average emission of NOx (orange), AVOC (blue), BVOC (green) during 2010 to 2016, respectively.